

Molecular docking and dynamic simulation of *Olea europaea* and *Curcuma Longa* compounds as potential drug agents for targeting Main-Protease of SARS-nCoV2

Rashid Saif^{1,2} * · Muhammad Hassan Raza¹ · Talha Rehman¹ · Muhammad Osama Zafar¹ · Saeeda Zia³ · Abdul Rasheed Qureshi⁴

¹ Institute of Biotechnology, Gulab Devi Educational Complex, Lahore, Pakistan.

² Decode Genomics, Punjab University Employees Housing Scheme (II), Lahore, Pakistan.

³ Department of Sciences and Humanities, National University of Computer and Emerging Sciences, Lahore, Pakistan.

⁴ Out-Patients Department-Pulmonology, Gulab Devi Chest Hospital, Ferozepur Road, Lahore, Pakistan.

**Corresponding author: Rashid Saif, Institute of Biotechnology, Gulab Devi Educational Complex, Lahore, Pakistan. Tel: +92-321-7107501 E-mail: rashid.saif37@gmail.com*

Abstract

One of the main reasons of rapidly growing cases of COVID-19 pandemic is the unavailability of approved therapeutic agents. Therefore, it is urgently required to find out the best drug by all means. Aim of the current study is to test the anti-viral drug potential of many of the available olive and turmeric compounds that can be used as potential inhibitors against one of the target proteins of SARS-nCoV2 named Main protease (Mpro/3CLpro). Molecular docking of thirty olive and turmeric compounds with target protein was performed using Molecular Operating Environment (MOE) software, out of these 19 ligands were selected for redocking using PyRx to validate MOE results and to determine the best ligand-protein interaction energies. Molecular dynamics simulation was performed on best 7 docked complexes by NAMD/VMD to determine the stability of the ligand-protein complex. Out of the thirty drug agents, 6 ligands do not follow the Lipinski rule of drug likeliness by violating two or more rules while remaining 24 obey the rules and included for the downstream analysis. We found that Demethyleoleuropein, Oleuropein, Rutin, Neuzhenide, Luteolin-7-rutinoside, Curcumin and Tetrahydrocurcumin gave best docking score and form much stable complexes during simulation. Our predictions suggest that these ligands have the potential inhibitory effects on Mpro of SARS-nCoV2, so, these herbal plants would be helpful in harnessing COVID-19 infection as home remedy with no serious known side effects. Further, in-vivo experimental studies are needed to validate the inhibitory properties of these compounds against the current and other target proteins in SARS-nCoV2.

Keywords *Curcuma longa* · COVID-19 · Main protease · Molecular docking · MOE software · PyRx · Molecular dynamic simulation · *Olea europaea* · SARS-nCoV2 · NAMD

1 Introduction

Coronaviruses (CoVs) are group of positive sense RNA viruses that cause upper respiratory tract infection, hepatic diseases, multiple organ failure and gastrointestinal disorder in both animals and humans (Brian and Baric 2005; Kupferschmidt 2013; Peiris et al. 2003; Renu et al. 2020).

In December 2019, patients with new kind of disease having symptoms like pneumonia were reported in Wuhan, Hubei Province of China (Lee and Hsueh 2020; Zhu et al. 2020). This infectious agent was recognized as a new strain of corona virus because it shares 70% similarity with SARS-CoV-1 (severe acute respiratory syndrome) and was temporarily given a name 2019-nCov (Hui et al. 2020). Virus has a characteristic human to human transmission and causes respiratory tract infection that ultimately leads to multiple organ failure (Paraskevis et al. 2020; Renu et al. 2020; Wang et al. 2020).

World Health Organization (WHO) officially named the virus as SARS-nCoV2 (disease COVID-19) and on March 31, 2020 declared the disease a pandemic (Cucinotta and Vanelli 2020). Until Jan 2021, COVID-19 caused more than 2.46M deaths and 111M confirmed cases worldwide ((WHO) 2020). SARS-nCoV2 (COVID-19) belongs to the family of *Coronaviridae* and is the seventh member of genus *Betacoronavirus* (Coronaviridae Study Group of the International Committee on Taxonomy of 2020).

SARS-nCoV2 infects the host cell by attaching to ACE-2 receptor through its spike protein (Renu et al. 2020). After binding, the virus moves into the cell and starts its replication. Besides spike protein, M^{pro} (main protease) / 3CL^{pro} and PL^{pro} (recognized as potential drug targets) also play main role in viral replication (Xu et al. 2020). Until now, there is no approved drug against COVID-19; however, supporting drugs like remdesivir, nelfinavir and hydroxychloroquine provide immunomodulatory action and prevents organ damage (Xu et al. 2020).

The main target of drugs against which scientists are focusing these days is M^{pro} (main protease), because main protease of SARS-nCoV2 shares 96% similarity with SARS-CoV-1 (Paraskevis et al. 2020). COVID-19's main target, M^{pro}/ 3CL^{pro}, has been successfully crystallized, submitted and repositioned in PDB (PDB ID: 6M2N) by Su *et al.* (2020). This protein represents a potential drug target and its inhibition results in the blockage of replication and infectious cycle of Corona virus (Xue et al. 2008).

Due to lack of specific drug against COVID-19, there is an ongoing trend of usage of herbs and herbal extracts because these are used as conventional antiviral medicines (Li and Peng 2013).

In present study, we will investigate the compounds of *Olea europaea* (olive) and *Curcuma longa* (turmeric) as the potential inhibitors of COVID-19 by computer-aided drug design (CADD) (Yu and MacKerell 2017). Molecular operating environment (MOE), PyRx and NAMD are used in this in-silico studies of Docking and MD Simulation. This investigation will provide other researchers the opportunity to identify best drugs to treat COVID-19.

2 Materials and Methods

2.1 Selection of Medicinal Herbs

2.1.1 *Olea europaea* (Olive)

Olea europaea, which is known for its great therapeutic potential, is widely recommended for treating COVID-19 infection because of its compounds, like *oleuropein*, that have antiviral properties (Micol et al. 2005). For centuries, it is being used in North African and Asian areas as a food and conventional medication due to Islamic conviction (Ali et al. 2018). *Olea europaea* extracts have antiviral, antiepileptic, antioxidant, anti-erythrocytic, germicide, cancer preventing, gastroprotective, wound mending, immunosuppressive, blood glucose lowering and pain relieving properties (Hashmi et al. 2015). Nearly its 25 bioactive compounds have been reported in olive extract as cited in different literatures (Boskou et al. 2015; Ghanbari et al. 2012; Hashmi et al. 2015). The structure of *Olea europaea* compounds are given in Fig. 1.

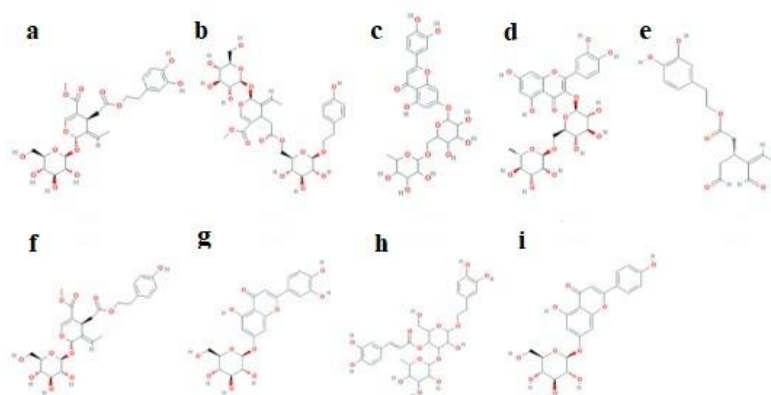


Fig. 1 Chemical structure of major compounds of *Olea europaea*. **a** Oleuropein **b** Neuzhenide **c** Luteolin 7-rutinoside **d** Rutin **e** Deacetoxyoleuropein aglycone **f** Ligstroside **g** Cynaroside (Luteolin-7-glucoside) **h** Verbascoside **i** Cosmosin

The chemical properties of compounds were taken from PubChem. Different scientist performed various experiments to obtain a set of properties and then submitted those in PubChem and other similar chemical databases. The chemical properties of *Olea europaea* compounds are given in (Table 1).

Table 1 The chemical parameters of *Olea europaea* compounds. TPSA= topological polar surface area, H-donn= hydrogen bond donor, H-acc= hydrogen bond acceptor, RB= rotatable bond

Ligands	Molecular Weight (g/mol)	PubChem CID	Toxicity	Log P	H-donn	H-acc	RB	TPSA	Molecular Formula
Oleuropein	540.5	5281544	NO	-0.4	6	13	11	202 Å ²	C ₂₅ H ₃₂ O ₁₃
Neuzhenide	686.7	6440999	NO	-2.2	8	17	14	261 Å ²	C ₃₁ H ₄₂ O ₁₇
luteolin 7rutinoside	594.5	12315422	NO	-1.1	9	15	6	245 Å ²	C ₂₇ H ₃₀ O ₁₅
Rutin	610.5	5280805	irritant	-1.3	10	16	6	266 Å ²	C ₂₇ H ₃₀ O ₁₆
Demethyloleoeuropein	526.5	6450302	NO	-0.8	7	13	10	213 Å ²	C ₂₄ H ₃₀ O ₁₃
Ligstroside	524.5	14136859	NO	-0.1	5	12	11	181 Å ²	C ₂₅ H ₃₂ O ₁₂
Verbascoside	624.6	354009	NO	-0.5	9	15	11	245 Å ²	C ₂₉ H ₃₆ O ₁₅
Cosmosin (apigenin 7-glucoside)	432.4	5280704	NO	-0.1	6	10	4	166 Å ²	C ₂₁ H ₂₀ O ₁₀
Luteolin	286.24	5280445	irritant	1.4	4	6	1	107 Å ²	C ₁₅ H ₁₀ O ₆
luteolin7glucoside	448.4	5280637	NO	0.5	7	11	4	186 Å ²	C ₂₁ H ₂₀ O ₁₁
Deacetoxyoleuropein aglycone	320.3	101102227	NO	1.1	2	6	10	101 Å ²	C ₁₇ H ₂₀ O ₆
Chlorogenic acid	354.31	1794427	irritant	-0.4	6	9	5	165 Å ²	C ₁₆ H ₁₈ O ₉
luteolin-4'-o-glucoside	448.4	5319116	NO	0.5	7	11	4	186 Å ²	C ₂₁ H ₂₀ O ₁₁
Apigenin	270.24	5280443	irritant	1.7	3	5	1	87 Å ²	C ₁₅ H ₁₀ O ₅
Quercetin	302.23	5280343	Irritant	1.5	5	7	1	127 Å ²	C ₁₅ H ₁₀ O ₇
Ferulic Acid	194.18	445858	Irritant	1.5	2	4	3	66.8 Å ²	C ₁₀ H ₁₀ O ₄
Flavylum	207.25	145858	NO	0	0	0	1	1 Å ²	C ₁₅ H ₁₁ O ⁺
Sinapic Acid	224.21	637775	irritant	1.5	2	5	4	76 Å ²	C ₁₁ H ₁₂ O ₅
Homovanillic Acid	182.17	1738	irritant	0.4	2	4	3	66.8 Å ²	C ₉ H ₁₀ O ₄
Cinamic Acid	255.4	5372020	NO	-0.6	2	5	6	114 Å ²	C ₁₁ H ₁₃ NO ₂ S ₂
Vanillic Acid	168.15	8468	irritant	1.4	2	4	2	66.8 Å ²	C ₈ H ₈ O ₄
Tyrosol	138.16	10393	irritant	0.4	2	2	2	40.5 Å ²	C ₈ H ₁₀ O ₂
Protocatehuic acid	154.12	72	Irritant	1.1	3	4	1	77.8 Å ²	C ₇ H ₆ O ₄
Hydroxytyrosol	154.16	82755	Irritant	-0.7	3	3	2	60.7 Å ²	C ₈ H ₁₀ O ₃
4-Hydroxy Benzoic Acid	138.12	135	Irritant	1.6	2	3	1	57.5 Å ²	C ₇ H ₆ O ₃

2.1.2 Curcuma longa (Turmeric)

Curcuma longa is known as a powerful natural healer. For quite a long time, it is being utilized in Asia as a traditional medicine (Bhowmik et al. 2008). Compounds in olive have antiviral, antineoplastic, antiprotozoal, microbicidal, fungicidal, COX-inhibitor, antioxidant and antivenin properties (Bhowmik et al. 2008). Five active compounds are present in turmeric (Chattopadhyay et al. 2003; Niranjana and Prof 2008) and their structures are given in Fig. 2.

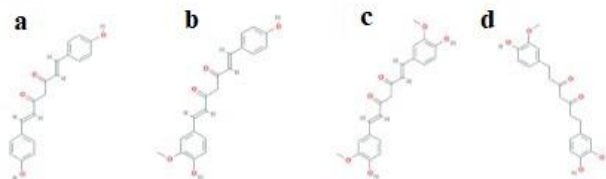


Fig. 2 The chemical structures of major compounds of *Curcuma longa*. **a** Bisdemethoxycurcumin **b** Demethoxycurcumin **c** Curcumin **d** Tetrahydrocurcumin

As *Curcuma longa* compounds are recognized for reducing effect of inflammation causing cytokinin (such as interleukin 6) but this herb is also reported for causing dermatitis. To predict drug potential, their properties are taken from PubChem database. The chemical properties of *Curcuma longa* compounds are given in (Table 2).

Table 2 Chemical properties of Turmeric compounds. TPSA= topological polar surface area, H-donn= hydrogen bond donor, H-acc= hydrogen bond acceptor, Env= environment, Haz= hazard

Ligands	Molecular Weight (g/mol)	PubChem CID	Toxicity	Log P	H-donn	H-acc	Biological Activity	TPSA	Molecular Formula
Curcumin	368.4	969516	irritant	3.2	2	6	Antibacterial, Antiviral	93.1Å ²	C ₂₁ H ₂₀ O ₆
Bisdemethoxycurcumin	308.3	5315472	irritant	3.3	2	4	Antioxidant	74.6Å ²	C ₁₉ H ₁₆ O ₄
Demethoxycurcumin	338.4	5469424	Env. Haz.	3.3	2	5	Antioxidant	83.8Å ²	C ₂₀ H ₁₈ O ₅
Tetrahydrocurcumin	372.4	124072	NO	2.8	2	6	Anti-inflammatory	93.1Å ²	C ₂₁ H ₂₄ O ₆
Ar-turmeron	216.32	160512	irritant	4	0	1	Antivenom	17.1Å ²	C ₁₅ H ₂₀ O

2.2 Selection of Targeted Protein

2.2.1 Main Protease

M^{pro}/3cl^{pro} (PDB ID: 6M2N) is the key enzyme in SARS-nCoV2 that has a main role in viral replication and transcription (Jin et al. 2020). This enzyme is involved in producing Nsps (non-structural proteins) which then assemble the viral protein. So by targeting M^{pro}, viral replication can be halted (Mengist et al. 2020).

Table 3 Crystallographic properties of enzyme (M^{Pro})

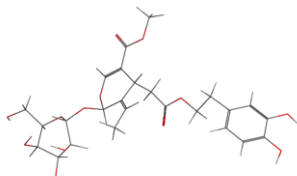
Enzyme	PDB ID	Classification	Virus	Expression system	Resolution	Method	Total structure weight (DA)	Chain	Atom count	Active site residues
Main protease	6M2N	Viral Protein	SARS-nCoV2 (Severe acute respiratory syndrome)	Escherichia coli BL21	2.20 Å	X-RAY Diffraction	136.38 kDa	A, B, C, D	9544	THR24, THR26, PHE140, ASN142, GLY143, CYS145, HIS163, HIS164, GLU166, HIS172

2.3 Molecular Docking using MOE

The molecular docking was performed by Molecular Operating Environment (MOE) software. It is a drug discovery software that can be used for checking protein-ligand interactions and for drug likeness analyses. MOE is a platform that incorporates visualization of results, modeling, simulations of structures and methodology development in one package (Vilar et al. 2008).

2.3.1 Preparation of Ligands

Several databases are available to obtain the desired ligand e.g. *DrugBank*, *Zinc*, *PubChem*, *Asinex*, *ChEMBL*, *Merck*, *Enamine* etc. These ligands can either be downloaded in sdf format or can be sketched in MOE interface by using *Builder Mode*. After sketching, the partial charges were added by using *compute* in MOE. Once the charges were added the prepared ligand is then saved as *MDB file* as shown in Fig. 3.

**Fig. 3** Prepared ligand of Oleuropein

2.3.2 Preparation of Target Protein

Protein data bank is the source of our target protein. PDB file 6M2N was downloaded and opened in MOE (Omar 2010).

a) Removal of Water, Inhibitor and Repeated Chains

The already attached ligand was removed to make active site accessible for new ligand. The water molecules were also removed from the protein surface so that the interacting region would not be hidden during docking. The repeated chains of M^{Pro} were also removed to avoid complications during docking.

b) Correction of Protein Structure

Errors and missing atoms in structure were then corrected and added by using the feature of *structure preparation* in MOE. For correction of structure, first Protein module of MOE was selected. Afterwards, by selecting *structure and*

preparation option, the new window appeared and from that *protonate 3D* module was selected and in the last step, the *correction* option corrected our desired protein's structure.

c) Active Site Finder

MOE main interface was used to open *compute* and after that *Site Finder* was selected. We chose *apply* option from new interface which gave number of different chains that could be the possible active site of target protein. From literature survey or Pymol, we selected the chain which had the sequence of active site residues. If the sequence of active site is unknown, then *blind docking* will prefer (it is better to use first 3 chains). *No Centers* and *atoms and backbone* option were selected from *Render* and *isolate* module respectively. Then by clicking *dummies* option, the dummy atoms were created. This prepared protein structure is displayed in Fig. 4.

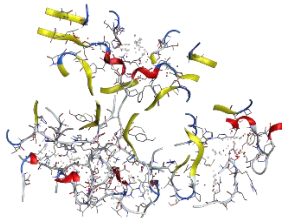


Fig. 4 Prepared protein (M-pro)

2.3.3 Docking and Surface Maps

Docking was performed to determine the possible interaction between ligand and active site of target protein 6M2N (Hewlings and Kalman 2017). A new dock window was opened when we selected *dock* from compute option in MOE interface. *Dummy atoms* in *site* module was selected (from which the docking was performed). We uploaded ligand file from *ligand mdb file* module which was previously prepared. In the end *command* was run. *Surface and maps* module in MOE focused and isolated the point where ligand attached to protein with minimum energy.

2.4 Redocking of molecules using PyRx

To further validate the results, it is necessary to perform docking with another software and for this purpose we selected PyRx which is virtual screening software incorporated with two built-in features and these are vina wizard (Auto-dock vina) to perform docking and open Babel to convert files (Dallakyan and Olson 2015). This PyRx works on graphical user interface

2.4.1 Protein Preparation

Protein of interest was first downloaded from protein data bank (PDB) and was further processed using following softwares

a) Pre-processing via DS

For pre-processing of protein, the discovery studio (DS) visualizer was used to remove all repeated chains, heteroatoms, water molecules and already attached ligand. Only chain of interest was remained at which active site was present, after deleting all unnecessary chains this file was saved as pdb format (Studio 2008).

b) Energy minimization by CHIMERA

The step of energy minimization and addition of hydrogen atoms is very crucial to obtain more stable conformer and to improve the local interaction in system (Pettersen et al. 2004). Already preprocessed file was loaded in UCSF CHIMERA by using directory. At first dock prep window was opened by using structure analysis option from tools section. Afterwards by clicking ok on dock prep window, another window was opened from which hydrogen atoms was added which lead to the opening of last window. To minimize energy and addition of charges AMBER

forcefield (AMBER ff14SB) and Gasteiger residue options was used respectively. The files we got was saved in PDB format.

2.4.2 Docking process

The redocking procedure was done by loading already prepared protein in PyRx. By using import option 2D-conformer of ligand was imported in SDF format. Before docking energy minimization of ligand was also done by using Universal force field (UFF) along with the conjugate gradient algorithm and total of 500 steps. Both molecules then converted in pdbqt format. In the last the Grid Box was arranged around active site of protein by using vina wizard option so that software only dock and search for maximum score in particular area within box. The docking result was obtained by using start option.

2.5 MD Simulation using VMD/NAMD

MD simulation was performed by using NAMD (Nanoscale Molecular Dynamics) to evaluate binding interactions of ligands with protein 6M2N. Already docked complexes with highest score are used for molecular dynamic simulation. NAMD software uses CHARMM36 force field (Phillips et al. 2005). Simulation of 1ns (nanosecond) is performed which is of 500,000 steps. Conjugate gradient method was used for energy minimization. Energy minimization was performed for 1000 steps by fixing the backbone atoms. Constant Temperature of 310K and pressure of 1ATM was used for the simulation of energy minimized structure using Periodic Boundary conditions. For further analysis the atomic coordinates of simulated structures were recorded at every 0.1 ps.

For MD simulation already docked complex must be modified, the coordinates of ligand with best pose (highest score) were inserted in protein file. Topologies of both protein and ligand were made after separating these two molecules from modified complexes by using VMD (Visual Molecular Dynamics) (Humphrey et al. 1996). This topology formation step was done to define atom types, bonds, and angles between atoms as well as the number of molecules in the simulation system. CHARMM-GUI web server were used to build Simulation inputs for ligand with CHARMM36 force field. Automatic PSF Generation within VMD program was used to convert Protein structure into Protein Structure File (PSF). By Merging both files after topology formation, solvation was performed to generate cubic water box around complex. By adjusting parameters (time, temperature, pressure, energy minimization steps and Periodic Boundary conditions) the final command of simulation was run on windows power-shell by using NAMD software.

3 Results

3.1 Docking Scores with MOE

3.1.1 Olea europaea

Molecular docking was done to estimate the ligand-protein interaction between different compounds of herbs and protein (main protease). The chance of ligand to be an effective drug increases with decrease of binding energy. The docking score of Olea europaea is given in (Table 4).

Table 4 Docking score Olive's compounds with 6M2N

SN	Ligands	Docking score (kcal/mol) with 6M2N
1	Neuzhenide	-10.9176493
2	Demethyloleoeuropein	-9.48762321
3	Rutin	-9.49832058
4	Oleuropein	-9.21493816
5	Luteolin 7-rutinoside	-9.18656158
6	Ligstroside	-8.72711468
7	Verbascoside	-8.5100832
8	Luteolin-7-glucoside	-7.68533516

9	Cosmosin	-7.67128038
10	luteolin-4'-o-glucoside	-7.25527763
11	Chlorogenic acid	-6.8014946
12	Deacetoxyoleuropein aglycone	-6.75398064
13	Leutolin	-6.27251291
14	Apigenin	-6.2212038
15	Quercetin	-6.00290871
16	Cinamic acid	-5.72288179
17	Sinapic acid	-5.69604254
18	Ferulic acid	-5.44703674
19	Homovanillic acid	-5.18638182
20	Flavylum	-5.05841064
21	Vanillic acid	-4.89071226
22	Hydroxytyrosol	-4.70743608
23	4-hydroxybenzoic	-4.65060616
24	Protocatehuic acid	-4.69090509
25	Tyrosol	-4.5343833

Graphical representation of scores of *Olea europaea* compounds are shown in Fig 5.

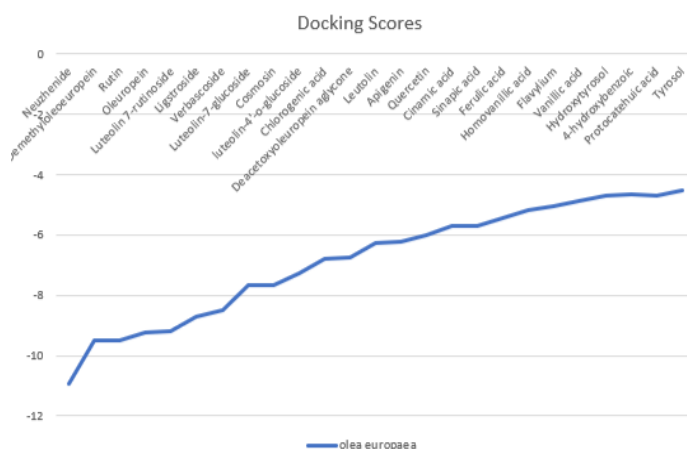


Fig. 5 Graphical representation of *Olea europaea* compounds scores

3.1.2 Curcuma Longa

The docking scores and graphical representation of *curcuma's longa* compounds are given in (Table 5) and Fig. 6 respectively. Curcumin gave the highest score with the binding energy of -7.6 kcal/mol. It is followed by Tetrahydrocurcumin and Demethoxycurcumin having energies of -7.4 and -7.02 respectively. Criteria based on docking scores selects the best compounds.

Table 5 Docking score Turmeric's compounds with 6M2N

SN	Ligands	Docking score (kcal/mol) with 6M2N
1	Curcumin	-7.65329599
2	Tetrehydrocurcumin	-7.42297649
3	Demethoxycurcumin	-7.02905893
4	Bidemethoxycurcumin	-6.77281666
5	Ar-Turmerone	-5.70936966

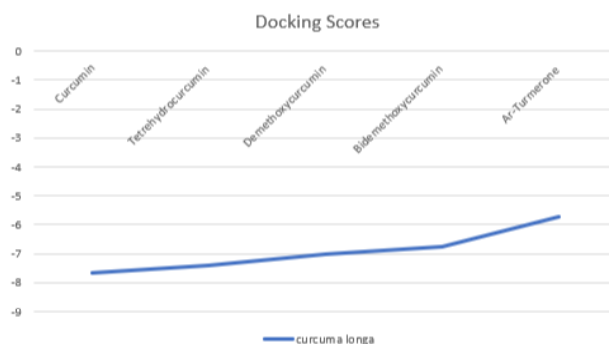


Fig. 6 Graphical representation of Curcuma longa compounds scores

3.2 Redocking scores with PyRx

For validation of docking protocol by MOE, redocking of crystal ligand with protein receptor (6M2N) was done by PyRx. Only ligands which gave the maximum results with Mpro by using MOE was redocked. Here we chose 15 ligands of olea europaea and 4 ligands of curcuma longa for further analysis. The redocking results are shown in (Table 6).

Table 6 Redocking results with PyRx

SN	Ligands of Olive and turmeric	Results by PyRx
1	Neuzhenide	-9.4
2	Demethyloleoeuropein	-8.1
3	Rutin	-9.5
4	Oleuropein	-6.6
5	Luteolin 7-rutinoside	-9.9
6	Ligstroside	-8.2
7	Verbascoside	-9.2
8	Luteolin-7-glucoside	-9.2
9	Cosmosin	-8.8
10	luteolin-4'-o-glucoside	-8.4
11	Chlorogenic acid	-7.6
12	Deacetoxyoleuropein aglycone	-6.1
13	Leutolin	-7.9
14	Apigenin	-7.6
15	Quercetin	-8.3
16	Curcumin	-7.2
17	Tetrahydrocurcumin	-6.8
18	Demethoxycurcumin	-6.5
19	Bidemethoxycurcumin	-7

3.3 Relationship of Lipinski's Rule and Ligand

According to Lipinski's rule of 5, the ligand which follows 2 or more rules can be considered as a good drug (Benet et al. 2016). We used the SwissADME tool (<http://www.swissadme.ch/index.php>) to determine how many ligands (which we used) in docking study were following Lipinski' rule.

3.3.1 Negation to Lipinski's Rule

There are total 7 ligands (Neuzhenide, Demethyloleoeuropein, Rutin, Oleuropein, Luteolin 7-rutinoside, Verbascoside) which violate 3 rules, but their energies range from -10 to -8.5 (-10.9176493, -9.48762321, -9.49832058, -9.21493816, -9.18656158, -8.5100832 respectively). The ligands shown in (Table 7) don't follow the Lipinski's rule.

Table 7 Ligands which do not follow Lipinski's rule

PubChem ID	Ligands	Molecular weight (<500Da)	LogP (<5)	H-Bond donor (5)	H-bond acceptor (<10)	Violations	Docking score
6440999	Neuzhenide	686.7	-2.2	8	17	3	-10.9176493
6450302	Demethyloleuropein	526.49	-0.8	7	13	3	-9.48762321
5280805	Rutin	610.5	-1.3	10	16	3	-9.49832058
5281544	Oleuropein	540.5	-0.4	6	13	3	-9.21493816
12315422	Luteolin 7-rutinoside	595.5	-1.1	9	15	3	-9.18656158
354009	Verbascoside	624.5	-0.5	9	15	3	-8.5100832

3.3.2 Ligands under Lipinski's Rule

There are total 24 ligands which follow Lipinski's rule of 5 and their energies range from -8.7 to -4.5. The drug scanning results show that all tested compounds in this study were accepted according to Lipinski's rule of five. Ligands which follow this rule are given in (Table 8).

Table 8 Ligands which follow Lipinski's rule

PubChem ID	Ligands	Molecular weight (<500Da)	LogP (<5)	H-Bond donor (5)	H-bond acceptor (<10)	Violations	Docking score
14136859	Ligstroside	524.5	-0.1	5	11	2	-8.72711468
5280637	Luteolin-7-glucoside	448.4	0.5	7	11	2	-7.68533516
5280704	Cosmosin	432.4	-0.1	6	10	1	-7.67128038
5319116	luteolin-4'-o-glucoside	448.4	0.5	7	11	2	-7.25527763
1794427	Chlorogenic acid	354.31	-0.4	6	9	1	-6.8014946
101102227	Deacetoxyoleuropein aglycone	320	1.1	2	6	0	-6.75398064
5280445	Leutolin	286.23	1.4	4	6	0	-6.27251291
5280443	Apigenin	270.24	1.7	3	5	0	-6.2212038
5280343	Quercetin	302.23	1.5	5	6	0	-6.00290871
5372020	Cinamic acid	255.54	-0.6	2	5	0	-5.72288179
637775	Sinapic acid	224.21	1.5	2	5	0	-5.69604254
445858	Ferulic acid	194.18	1.5	2	4	0	-5.44703674
1738	Homovanillic acid	182.17	0.4	2	4	0	-5.18638182
145858	Flavylum	207.25	0	0	1	0	-5.05841064
8468	Vanillic acid	168.15	1.4	2	4	0	-4.89071226
82755	Hydroxytyrosol	154.16	-0.7	3	3	0	-4.70743608
135	4-hydroxybenzoic	138.12	1.6	2	3	0	-4.65060616
72	Protocatehuic acid	154.12	1.1	3	4	0	-4.69090509
10393	Tyrosol	138.16	0.4	2	2	0	-4.5343833
969516	Curcumin	368.4	3.2	2	6	0	-7.65329599
124072	Tetrehydrocurcumin	372.4	2.8	2	6	0	-7.42297649
5469424	Demethoxycurcumin	338.4	3.2	2	5	0	-7.02905893
5315472	Bidemethoxycurcumin	308.4	3.3	2	4	0	-6.77281666
160512	Ar- turmerone	216.32	4	0	1	0	-5.70936966

3.4 Ligands with Best Binding Energies

When docked, the ligand attached to the active site of 3CL^{pro}/M^{pro} and can be visualized by ligand and interaction module for 2D structure and surface and maps module for 3D structure of MOE. Docking results from (Table 4 and

5) show Neuzhenide from olive and Curcumin from turmeric give the lowest energy i.e. (-10.9176493 Kcal/mol) and (-7.65329599) respectively. Through MOE *ligand interactions* module, the binding pattern can be visualized.

3.4.1 Best Ligands of *Olea europaea*

Neuzhenide, when docked with 6M2N, showed two hydrogen possible interactions with amino acid LEU B282 (H-donor) with distance of 2.85Å and energy of -1.4 and amino acid GLU B288 (H-donor) with distance of 2.89Å and energy of -0.9 kcal/mol shown in Fig. 7.

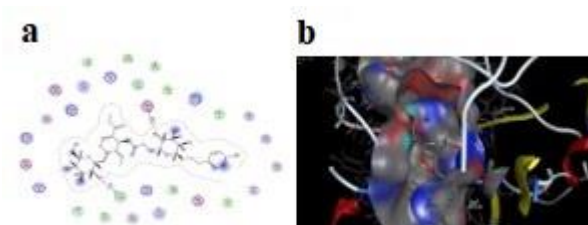
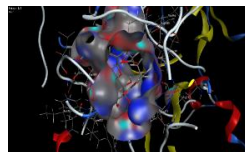
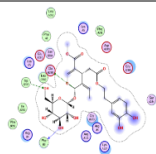


Fig. 7 a Ligand interaction of 6M2N with Neuzhenide b 3D diagram of pocket 6M2N with Neuzhenide

The interaction usually describes that how much a ligand can form a stabilized bond with target protein. Low binding energy leads to the formation of stabilized bond which give possibility for ligand to be an effective inhibitor. Interaction of other major ligands of *Olea europaea* whom energies range from -10 to -6 are given in (Table 9).

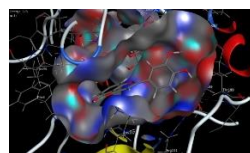
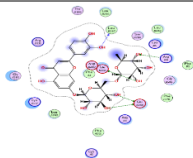
Table 9 Interaction of major ligands of Olive

Demethyleuropein	
Four hydrogen interaction are possible (a) Amino acid PHE 3 (H-donor) distance 3.06Å ⁰ and energy of -0.9kcal/mol (b) Amino acid LEU 282 (H-donor) distance 2.97Å ⁰ and energy of -2.1kcal/mol (c) Amino acid GLU 288 (H-donor) distance 2.87Å ⁰ and energy of -1.7kcal/mol (d) Amino acid LYS 137 (π-H) distance 3.84Å ⁰ and energy of -0.7kcal/mol	
Rutin	
Six hydrogen interactions are possible (a) Amino acid LEU 282 (H-donor) distance 3.44Å ⁰ and energy -0.7kcal/mol (b) Amino acid GLU 288 (H-donor) distance 2.80Å ⁰ and energy -4.1kcal/mol (c) Amino acid ASP 289 (H-donor) distance 3.06Å ⁰ and energy -2.3kcal/mol (d) Amino acid GLU 288 (H-donor) distance 2.75Å ⁰ and energy -1.5kcal/mol (e) Amino acid TRP 207 (H-acceptor) distance 3.13Å ⁰ and energy -1.3kcal/mol (f) Amino acid LYS 5 H-acceptor distance 2.80Å ⁰ and energy -1.7kcal/mol	
Oleuropein	



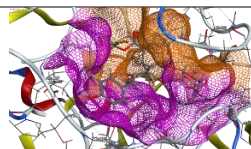
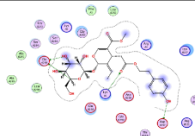
Three hydrogen interactions are possible (a) Amino acid GLU 288 (H-donor) distance 3.38\AA and energy -1.0kcal/mol (b) Amino acid PHE 3 (H-donor) distance 2.63\AA and energy -2.7kcal/mol (c) Amino acid TRP 207 (H-acceptor) distance 2.87\AA and energy -1.8kcal/mol

Luteolin 7-rutinoside



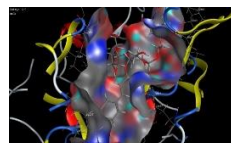
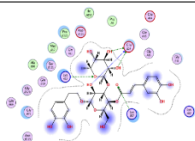
Five type of hydrogen interactions are possible (a) Amino acid LEU 287 (H-donor) distance 2.83\AA energy of -0.7kcal/mol (b) Amino acid GLU 288 (H-donor) distance 2.93\AA energy of -1.4kcal/mol (c) Amino acid GLU 288 (H-donor) distance 2.80\AA energy of -3.4kcal/mol (d) Amino acid GLU 288 (H-donor) distance 3.00\AA energy of -1.4kcal/mol (e) Amino acid ARG 4 (H-acceptor) distance 3.34\AA energy of -1.2kcal/mol

Ligstroside



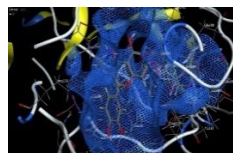
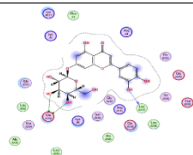
Four types of hydrogen interactions are possible (a) Amino acid GLU 288 (H-donor) distance 3.26\AA energy of -0.8kcal/mol (a) Amino acid GLU 288 (H-donor) distance 2.87\AA energy of -4.0kcal/mol (b) Amino acid ASP 197 (H-donor) distance 3.11\AA energy -1.3kcal/mol (c) Amino acid LYS 5 (H-acceptor) distance 3.04\AA energy -4.7kcal/mol

Verbascoside



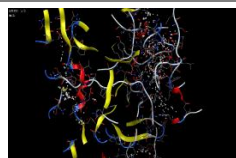
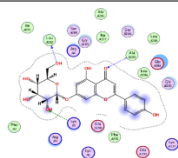
Five types of hydrogen interactions are possible (a) Amino acid GLU 14 (H-donor) distance 3.06\AA energy of -1.5kcal/mol (b) Amino acid GLU 14 (H-donor) distance 2.75\AA energy of -4.5kcal/mol (c) Amino acid GLU 14 (H-donor) distance 2.83\AA energy of -2.0kcal/mol (d) Amino acid LYS 12 (H-acceptor) distance 3.23\AA energy of -3.4kcal/mol (e) Amino acid LYS 97 (H-acceptor) distance 3.24\AA energy of -1.2kcal/mol

Luteolin-7-glucoside



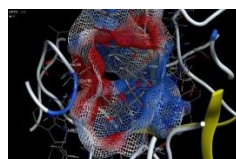
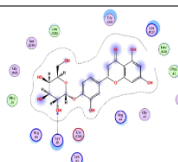
Three types of hydrogen interaction are possible (a) Amino acid GLU 288 (H-donor) distance 2.81\AA energy of -4.4kcal/mol (b) Amino acid GLU 288 (H-donor) distance 3.14\AA energy of -2.4kcal/mol (c) Amino acid LEU 287 (H-donor) distance 2.94\AA energy of -1.0kcal/mol

Cosmosin



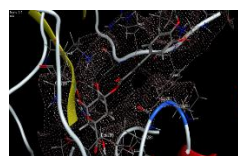
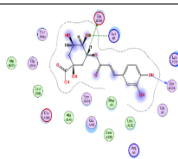
Three hydrogen interactions are possible (a) Amino acid LEU 282 (H-donor) distance 2.87\AA energy of -1.2kcal/mol (b) Amino acid ALA 285 (H-acceptor) distance 3.41\AA energy of -0.9kcal/mol (c) Amino acid LYS 5 (H-acceptor) distance 3.34\AA energy of -0.5kcal/mol

Luteolin-4'-O-glucoside



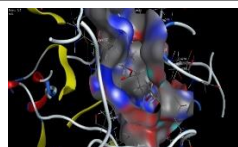
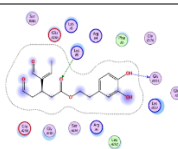
One type of hydrogen interaction is possible (a) Amino acid LYS 5 (H-acceptor) distance 3.29\AA energy of -1.1kcal/mol

Chlorogenic acid



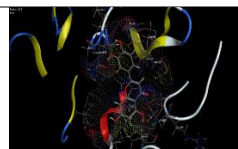
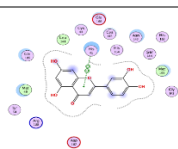
Three types of hydrogen interactions are possible (a) Amino acid GLU 288 (H-donor) distance 3.59\AA energy of -0.7kcal/mol (b) Amino acid GLY 138 (H-donor) distance 3.06\AA energy of -2.5kcal/mol (c) Amino acid LYS 5 (H-acceptor) distance 3.27\AA energy of -0.6kcal/mol

Deacetoxyoleuropein aglycone



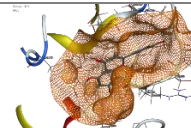
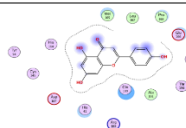
Two types of hydrogen interactions are possible (a) Amino acid GLY 138 (H-donor) distance 3.11\AA energy of -2.4kcal/mol (b) Amino acid LYS 5 (H-acceptor) distance 3.06\AA energy of -1.6kcal/mol

Leutolin



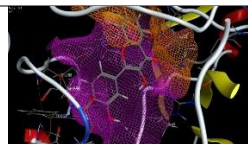
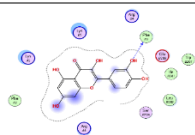
one type of hydrogen interaction is possible (a) Amino acid HIS 41 ($\pi - \pi$) distance 3.83\AA energy of -0.0kcal/mol

Apigenin



No perceptible interactions, only electrostatics exist (Van der Waals)

Quercetin



one type of hydrogen interaction is possible (a) Amino acid PHE 3 (H-donor) distance 2.92\AA energy of -1.7kcal/mol

3.4.2 Best Ligands of *Curcuma longa*

Curcumin, when docked with 6M2N, showed one hydrogen possible interaction with amino acid GLU C290 with distance of 2.83\AA and energy of -0.8 kcal/mol . This interaction is shown in Fig. 8.

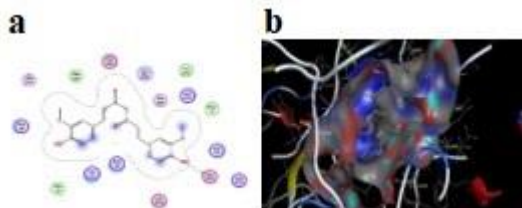
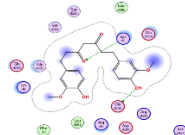
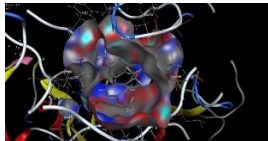
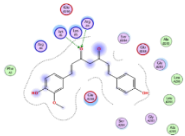
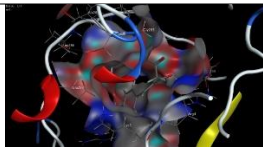


Fig. 8 a Ligand interaction of 6M2N with Curcumin b 3D diagram of pocket 6M2N with Curcumin

Curcuma longa ligands gave the lower score as compared to major *Olea europaea* compounds. But these ligands have great potential to inhibit viral activity of SARS-nCoV2. The interactions of major ligands of *Curcuma longa* (other than curcumin) whom energies are from -7 to -6 are given in (Table 10).

Table 10 Interaction of major ligands of Turmeric

Tetrehydrocurcumin	
	
Two types of hydrogen interactions are possible (a) Amino acid GLU 290 (H-donor) distance 2.86\AA energy -2.6kcal/mol (a) Amino acid LYS 5 (H-acceptor) distance 3.30\AA energy -1.4kcal/mol	
Demethoxycurcumin	
	
Two types of hydrogen interactions are possible (a) Amino acid LYS A5 (H-accepter) distance 2.53\AA energy of -1.3kcal/mol (b) Amino acid ARG B4 (H-accepter) distance 2.3\AA energy of -1.2kcal/mol	
Bidemethoxycurcumin	



Two types of hydrogen interactions are possible (a) Amino acid LYS B5 (H-accepter) distance 2.1\AA energy of -0.9kcal/mol (b) Amino acid LYS B4 (H-accepter) distance 1.9\AA energy of -1.4kcal/mol

4 Molecular Dynamic Simulation Analysis

Molecular dynamic simulation was performed to evaluate the stability of structure obtained from molecular docking studies. The analysis of molecular dynamic simulation was subjected to ligands which gave highest score with docking and redocking. By comparing the results of docking from both MOE and PyRx, we screened 5 complexes (ligand with Mpro) (Neuzhenide, Demethyleoleuropein, Rutin, Oleuropein, Luteolin 7-rutinoside) of *olea europaea* and 2 complexes (Curcumin, Tetrahydrocurcumin) of *curcuma longa* for simulation. This evaluation with simulation was performed for 1ns. The aim of this simulation was to check whether the docked poses in highest scored complexes remained stable.

4.1 RMSD calculation

RMSD (root mean square deviation) calculations was done to measures the average distance between groups of atoms. This was done by using VMD (Visual Molecular Dynamics). The RMSD plot of *olea europaea* complexes shown in figure. Demethyleoleuropein RMSD plot shows that docked complex remained stable from 270 frames to 3000 frames (nearly 0.25ns to 0.75ns) at 2\AA , then slightly increased and become persistent at 2.5\AA from 3000 frames till end of run. Results of Rutin complex indicates that the complex reaches stability at 2\AA from 200 frames till 1300 frames of the simulation, the RMSD value decrease up to 1.5\AA and again becomes stable till the end of run. RMSD graph of oleuropein remain nearly same as Rutin where it got stable for short intervals at 1.5\AA then it its value decreases to 1.25\AA and deviate at the end of simulation. The plot of last two complexes Luteolin 7-rutinoside and Neuzhenide keep on fluctuating irregularly and remain stable for short interval of time between 1750 frames to 2750 frames at 1.5\AA and from 1100 frames to 2100 frames at 1.5\AA respectively.

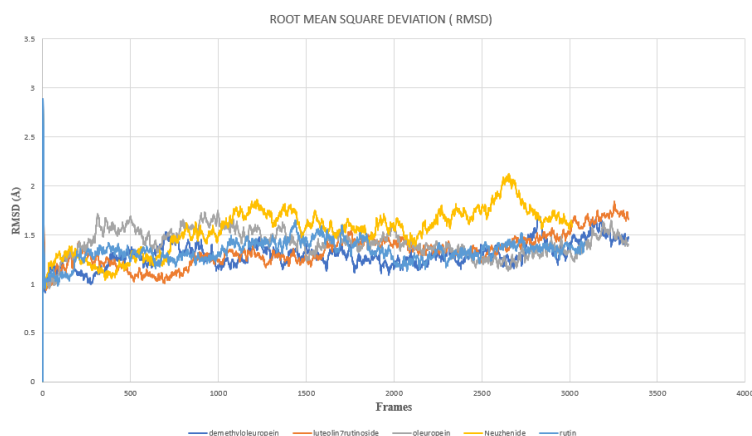


Fig. 9 RMSD graph of *olea europaea* docked complex

The RMSD plot of *curcuma longa* complexes are shown in figure, where graph of docked complex Tetrahydrocurcumin remained stable throughout the course of simulation at 1.25\AA , a slight deviation is seen at the end where is decrease to 1.1\AA . The plot of curcumin only has slight variation in start with continuously increasing, after that it remain stable at the end at 1.5\AA .

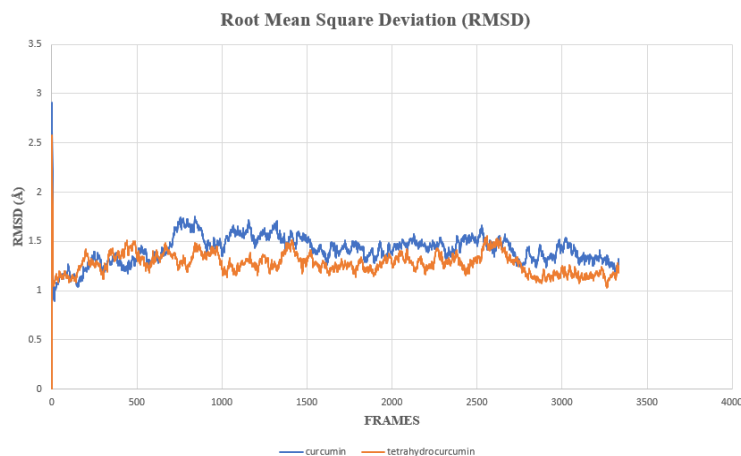


Fig. 10 RMSD plot of curcuma longa docked complex

4.2 H-bond analysis

Hydrogen bond analysis during molecular dynamic simulation complexes of olea europaea and curcuma longa are shown in figures respectively. The gap between two residues are reduced by the formation of strong hydrogen bond with water. In Demethyleoleuropein complex of olea europaea, total 13 hydrogen bonds are formed, major hydrogen bond which is responsible for stabilization of complex make occupancy rate of 69% and between major ligand (act as donor) and aspartic acid ASP-289 (act as receptor). In simulation of Luteolin 7-rutinoside out of 20 hydrogen bonds, bond with ligand (ligand) and glutamic acid GLU288 (acceptor) with occupancy rate of 77.39% is responsible for stabilization. In simulation Oleuropein complex was stable due to formation of hydrogen bond of ligand (donor) and aspartic acid ASP153 (acceptor) which remained 96.28% of simulation time. Neuzhenide complex was stable by forming hydrogen bond between ligand (donor) and aspartic acid ASP289-Side (acceptor) and remained stable for 81.74% of simulation run. Simulation of Rutin complex was stabilized by hydrogen bond of ligand (donor) and aspartic acid ASP289 (acceptor) with the occupancy of 79.68%.

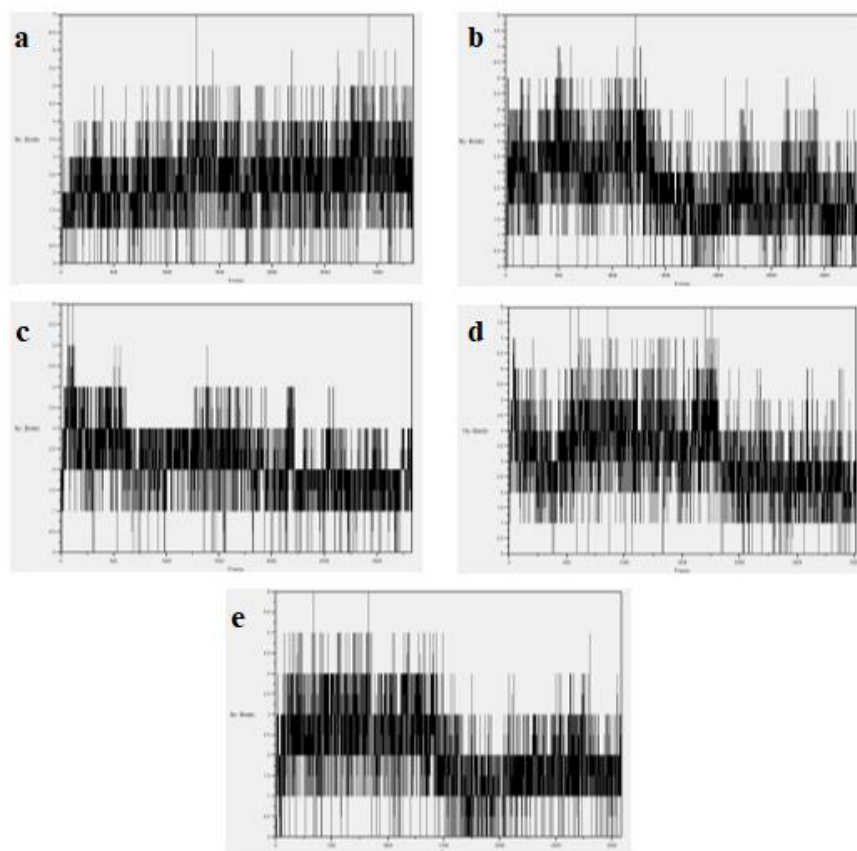


Fig. 11 H-bonds graph of olea europaea docked complex **a** Demethyloleoeuropein **b** Luteolin 7-rutinoside **c** Oleuropein **d** Neuzhenide **e** Rutin

While in complexes of curcuma longa, curcumin and Tetrahydrocurcumin got stabilize with 71.90% bond formation between lysine LYS5-Main (donor) and ligand (acceptor) and 38.74% bond formation with lysine LYS137-Side (donor) and ligand (receptor) respectively as shown in Fig. 12.

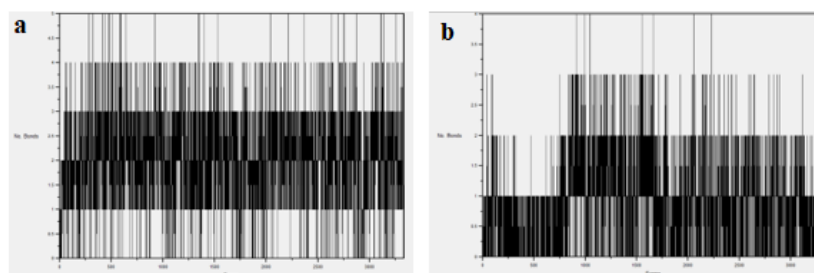


Fig. 12 H-bonds graph of curcuma longa docked complex **a** Curcumin **b** Tetrahydrocurcumin

4.3 Heat map plot

Heat map of both olea europaea and curcuma longa complexes can be seen in Fig. 13 and 14, made by RMSD visualizer tool built-in feature of VMD, these heat signatures shows the stability of complexes during simulation. In the heatmap graph of Olea europaea complexes Demethyloleoeuropein, Oleuropein and Rutin shows promising stability where neuzhenide and luteolin-7-rutinoside show low stability of short intervals.

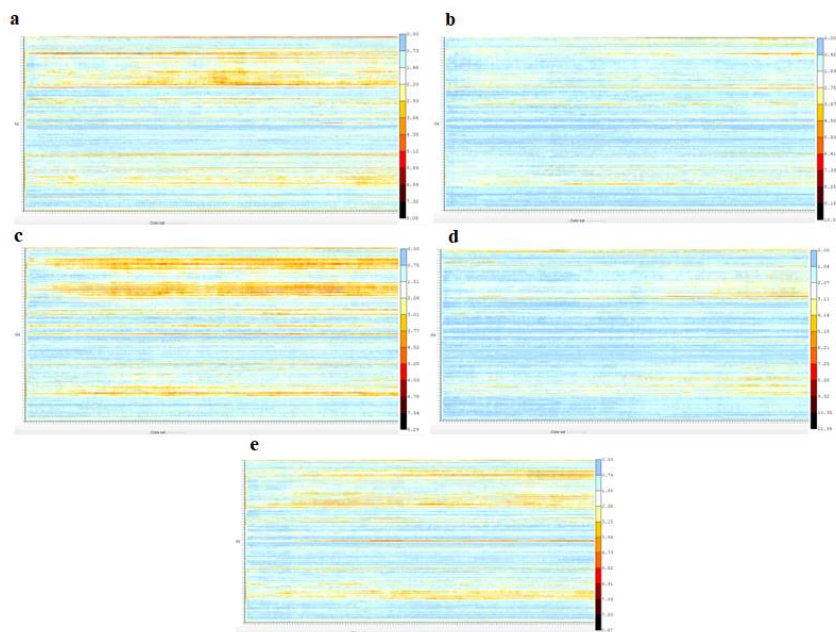


Fig. 13 heat map of olea europaea **a** Demethyloleoeuropein **b** Luteolin 7-rutinoside **c** Oleuropein **d** Neuzhenide **e** Rutin

In cursuma longa complexes, curuma is far stable than tetrahydrocurcumin, which has low stability.

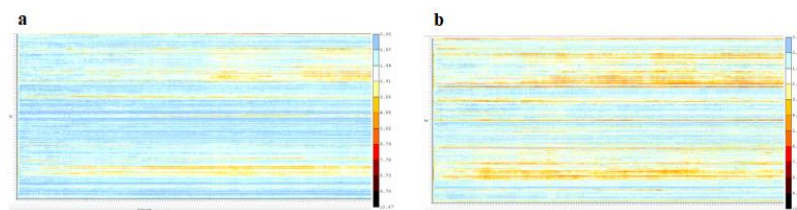


Fig. 14 heat map of curcuma longa **a** Curcumin **b** Tetrahydrocurcumin

5 Discussion

To our knowledge, this kind of drug finding research on COVID-19 is limited. A number of barriers have been identified and out of these barriers, the most prominent one is mutation (Pachetti et al. 2020), as SARS-nCoV2 is RNA virus that mutates very quickly making its drug or vaccine less affective (Burton and Walker 2020). The present study focuses on finding potential drug of SARS-nCoV2 using docking study and molecular dynamic simulation. The main protein target here is SARS-nCoV2 main protease (M^{pro} / 3cl-protease) which is required for viral replication and maturation. By blocking this protein, the further replication of virus can be halted.

Major findings are Rutin, Demethyloleoeuropein and Oleuropein from natural source of olea europaea and Curcumin from curcuma longa which after docking, redocking and molecular dynamic studies gave lowest energy as compare to other ligands that form stable protein-ligand complex with lowest energy by accurately fitting in active site of M-protease and forming the maximum hydrogen bonds, also made the most stable complex with M-protease during molecular dynamic simulation run. In contrast Neuzhenide and Luteolin-7-rutinoside from Olea europaea and Tetrahydrocurcumin from Curcuma longa also gave the minimum energy but fluctuate randomly and remain stable for short interval during simulation. These findings are important because these compounds can be the potential inhibitors of SARS-nCoV2, as molecular docking and molecular dynamic simulation predicts protein-ligand interaction and stability and is used in computer aided drug designing.

Drugs which are currently recommended in COVID-19 (nelfinavir, remdesivir and hydroxychloroquine) show the ligand-protein interaction docking score of -9.18 kcal/mol, -6.3 kcal/mol and -5.7 kcal/mol respectively in different articles (Bouchentouf and Nouredine 2020; Khaerunnisa et al. 2020). The ligands of olive and turmeric gave high docking score and are more stable in comparison to these recommended drugs.

The Neuzhenide, Oleuropein and Demethyloleuropein are nontoxic when their properties were checked from SwissADME and can be used without any harmful effects. Oleuropein has antiviral property and is currently used to treat infectious mononucleosis, epidemic jaundice, diarrheal disease, bovine rhinovirus infection, canine parvovirus infection and feline leukemia (Omar 2010). Pharmacological properties of Oleuropein include anti-irritant, antiangiogenic, anti-malignancy, antimicrobial and cytoprotective. Rutin, a flavonoid compound, has several biological activities like antiallergic, antitumor, reduce inflammation and antiangiogenic (Ganeshpurkar and Saluja 2017). Luteolin 7-rutinoside has a number of different properties and the most promising ones are antiallergic, antimicrobial, antimutagenic and anticarcinogenic activities (Hewlings and Kalman 2017). *Curcuma longa* compound Curcumin is a phytopolyphenol pigment, which blocks the formation of reactive-oxygen species and possesses antineoplastic and anti-inflammatory properties (Hewlings and Kalman 2017).

There are few limitations related to Lipinski's rule of drug likeness. As given in table 8 and 9, there are 6 ligands that do not follow Lipinski's rule, but their scores are between -10 and -7 kcal/mol while 24 ligands follow Lipinski's rule, scoring from -7 to -4 kcal/mol. But several articles reported that Lipinski's rule does not apply on natural products and semisynthetic natural drugs (Zhang and Wilkinson 2007). Furthermore, the recommended drug remdesivir and many other drugs that are currently being used in COVID-19 do not follow Lipinski's rule.

As research in this field is lacking and there is a desperate need to design an effective drug against COVID-19 in this pandemic, so Demethyloleuropein, Rutin, Oleuropein and curcumin can be the potential inhibitors of COVID-19 as they gave the best docking scores and maximum stability with M-protease. Neuzhenide, , Luteolin 7-rutinoside, Ligstroside, Verbascoside, Luteolin-7-glucoside, Curcumin, Tetrahydrocurcumin and Demethoxycurcumin can also be consider for drug designing. As a result, these olive and turmeric ligands are recommended for future research.

6 Conclusions

In the current scenario of COVID-19 pandemic, where near to 2.5 million people died and more than 111 million people are affected till now, there is no approved drug against COVID-19. Computer-aided drug designing (CADD) can help to overcome this situation through ligand-protein interaction (docking) and simulation studies. The aim of this study was to examine compounds from olive and turmeric that can be used to inhibit SARS-nCoV2 by acting on one of its enzymes, Main protease (M-pro), which is essential for viral replication. Molecular docking and molecular dynamic simulation results show that Demethyloleuropein, Rutin, Oleuropein, Neuzhenide and Curcumin gave the lowest binding energies and stable complex during simulation from olive and turmeric and are the most recommended ones against COVID-19. These suggested inhibitors are necessary to be investigated in further research and clinical trials to determine their action against SARS-nCoV2.

Acknowledgements

Authors acknowledge the great efforts of the institutes involved in databases and MOE software development.

Compliance with ethical standards

There is no ethical statement required as raw data was taken from publicly available databases.

Conflict of interests

The authors declare no conflict of interest.

References

- (WHO) WHO (2020) covid-19 statistics, https://www.who.int/docs/default-source/coronaviruse/situation-reports/20200805-covid-19-sitrep-198.pdf?sfvrsn=f99d1754_2.
- Ali SA, Parveen N, Ali AS (2018) Links between the Prophet Muhammad (PBUH) recommended foods and disease management: A review in the light of modern superfoods Int J Health Sci (Qassim) 12:61-69
- Benet LZ, Hosey CM, Ursu O, Oprea TI (2016) BDDCS, the Rule of 5 and drugability Adv Drug Deliv Rev 101:89-98 doi:10.1016/j.addr.2016.05.007
- Bhowmik D, Kumar K, Chandira M, Jayakar B (2008) Turmeric: A Herbal and Traditional Medicine Arch Appl Sci Res 1
- Boskou D, Camposeo S, Clodoveo ML (2015) 8 - Table Olives as Sources of Bioactive Compounds. In: Boskou D (ed) Olive and Olive Oil Bioactive Constituents. AOCS Press, pp 217-259. doi:<https://doi.org/10.1016/B978-1-63067-041-2.50014-8>
- Bouchentouf S, Noureddine M (2020) Identification of Compounds from Nigella Sativa as New Potential Inhibitors of 2019 Novel Coronavirus (Covid-19): Molecular Docking Study. doi:10.26434/chemrxiv.12055716.v1
- Brian DA, Baric RS (2005) Coronavirus Genome Structure and Replication. In: Enjuanes L (ed) Coronavirus Replication and Reverse Genetics. Springer Berlin Heidelberg, Berlin, Heidelberg, pp 1-30. doi:10.1007/3-540-26765-4_1
- Burton DR, Walker LM (2020) Rational Vaccine Design in the Time of COVID-19 Cell Host & Microbe 27:695-698 doi:<https://doi.org/10.1016/j.chom.2020.04.022>
- Chattopadhyay I, Biswas K, Bandyopadhyay U, Banerjee R (2003) Turmeric and Curcumin: Biological actions and medicinal applications Curr Sci 87
- Coronaviridae Study Group of the International Committee on Taxonomy of V (2020) The species Severe acute respiratory syndrome-related coronavirus: classifying 2019-nCoV and naming it SARS-CoV-2 Nat Microbiol 5:536-544 doi:10.1038/s41564-020-0695-z
- Cucinotta D, Vanelli M (2020) WHO Declares COVID-19 a Pandemic Acta bio-medica : Atenei Parmensis 91:157-160 doi:10.23750/abm.v91i1.9397
- Dallakyan S, Olson AJ (2015) Small-molecule library screening by docking with PyRx Methods Mol Biol 1263:243-250 doi:10.1007/978-1-4939-2269-7_19
- Ganeshpurkar A, Saluja AK (2017) The Pharmacological Potential of Rutin Saudi Pharm J 25:149-164 doi:10.1016/j.jsps.2016.04.025
- Ghanbari R, Anwar F, Alkharfy KM, Gilani AH, Saari N (2012) Valuable nutrients and functional bioactives in different parts of olive (Olea europaea L.)-a review International journal of molecular sciences 13:3291-3340 doi:10.3390/ijms13033291
- Hashmi MA, Khan A, Hanif M, Farooq U, Perveen S (2015) Traditional Uses, Phytochemistry, and Pharmacology of <i>Olea europaea</i> (Olive) Evidence-Based Complementary and Alternative Medicine 2015:541591 doi:10.1155/2015/541591
- Hewlings SJ, Kalman DS (2017) Curcumin: A Review of Its' Effects on Human Health Foods 6:92 doi:10.3390/foods6100092
- Hui DS et al. (2020) The continuing 2019-nCoV epidemic threat of novel coronaviruses to global health — The latest 2019 novel coronavirus outbreak in Wuhan, China International Journal of Infectious Diseases 91:264-266 doi:10.1016/j.ijid.2020.01.009
- Humphrey W, Dalke A, Schulten KJJomg (1996) VMD: visual molecular dynamics 14:33-38
- Jin Z et al. (2020) Structure of Mpro from SARS-CoV-2 and discovery of its inhibitors Nature 582:289-293 doi:10.1038/s41586-020-2223-y
- Khaerunnisa S, Kurniawan H, Awaluddin R, Suhartati S, Soetjipto S (2020) Potential Inhibitor of COVID-19 Main Protease (Mpro) From Several Medicinal Plant Compounds by Molecular Docking Study. doi:10.20944/preprints202003.0226.v1
- Kupferschmidt K (2013) Emerging diseases. Researchers scramble to understand camel connection to MERS Science (New York, NY) 341:702 doi:10.1126/science.341.6147.702
- Lee P-I, Hsueh P-R (2020) Emerging threats from zoonotic coronaviruses-from SARS and MERS to 2019-nCoV J Microbiol Immunol Infect 53:365-367 doi:10.1016/j.jmii.2020.02.001
- Li T, Peng T (2013) Traditional Chinese herbal medicine as a source of molecules with antiviral activity Antiviral Research 97:1-9 doi:<https://doi.org/10.1016/j.antiviral.2012.10.006>
- Mengist HM, Fan X, Jin T (2020) Designing of improved drugs for COVID-19: Crystal structure of SARS-CoV-2 main protease Mpro Signal Transduction and Targeted Therapy 5:67 doi:10.1038/s41392-020-0178-y

- Micol V, Caturla N, Pérez-Fons L, Más V, Pérez L, Estepa A (2005) The olive leaf extract exhibits antiviral activity against viral haemorrhagic septicaemia rhabdovirus (VHSV) *Antiviral Res* 66:129-136 doi:10.1016/j.antiviral.2005.02.005
- Niranjan A, Prof D (2008) Chemical constituents and biological activities of turmeric (*Curcuma longa* L.) -A review *Journal of Food Science and Technology* 45:109-116
- Omar SH (2010) Oleuropein in olive and its pharmacological effects *Sci Pharm* 78:133-154 doi:10.3797/scipharm.0912-18
- Pachetti M et al. (2020) Emerging SARS-CoV-2 mutation hot spots include a novel RNA-dependent-RNA polymerase variant *Journal of Translational Medicine* 18:179 doi:10.1186/s12967-020-02344-6
- Paraskevis D, Kostaki EG, Magiorkinis G, Panayiotakopoulos G, Sourvinos G, Tsiodras S (2020) Full-genome evolutionary analysis of the novel corona virus (2019-nCoV) rejects the hypothesis of emergence as a result of a recent recombination event *Infect Genet Evol* 79:104212-104212 doi:10.1016/j.meegid.2020.104212
- Peiris JS et al. (2003) Coronavirus as a possible cause of severe acute respiratory syndrome *Lancet* (London, England) 361:1319-1325 doi:10.1016/S0140-6736(03)13077-2
- Pettersen EF, Goddard TD, Huang CC, Couch GS, Greenblatt DM, Meng EC, Ferrin TEJ (2004) UCSF Chimera—a visualization system for exploratory research and analysis 25:1605-1612
- Phillips JC et al. (2005) Scalable molecular dynamics with NAMD *Journal of computational chemistry* 26:1781-1802 doi:10.1002/jcc.20289
- Renu K, Prasanna PL, Valsala Gopalakrishnan A (2020) Coronaviruses pathogenesis, comorbidities and multi-organ damage - A review *Life Sci* 255:117839-117839 doi:10.1016/j.lfs.2020.117839
- Studio DJA (2008) Discovery Studio
- Vilar S, Cozza G, Moro S (2008) Medicinal Chemistry and the Molecular Operating Environment (MOE): Application of QSAR and Molecular Docking to Drug Discovery *Current topics in medicinal chemistry* 8:1555-1572 doi:10.2174/156802608786786624
- Wang T, Du Z, Zhu F, Cao Z, An Y, Gao Y, Jiang B (2020) Comorbidities and multi-organ injuries in the treatment of COVID-19 *The Lancet* 395:e52 doi:10.1016/S0140-6736(20)30558-4
- Xu Z, Peng C, Shi Y, Zhu Z, Mu K, Wang X, Zhu W (2020) Nelfinavir was predicted to be a potential inhibitor of 2019-nCoV main protease by an integrative approach combining homology modelling, molecular docking and binding free energy calculation:2020.2001.2027.921627 doi:10.1101/2020.01.27.921627 %J bioRxiv
- Xue X et al. (2008) Structures of Two Coronavirus Main Proteases: Implications for Substrate Binding and Antiviral Drug Design 82:2515-2527 doi:10.1128/JVI.02114-07 %J *Journal of Virology*
- Yu W, MacKerell AD, Jr. (2017) Computer-Aided Drug Design *Methods Mol Biol* 1520:85-106 doi:10.1007/978-1-4939-6634-9_5
- Zhang MQ, Wilkinson B (2007) Drug discovery beyond the 'rule-of-five' *Current opinion in biotechnology* 18:478-488 doi:10.1016/j.copbio.2007.10.005
- Zhu N et al. (2020) A Novel Coronavirus from Patients with Pneumonia in China, 2019 *The New England journal of medicine* 382:727-733 doi:10.1056/NEJMoa2001017